

CHEM MED CHEM

CHEMISTRY ENABLING DRUG DISCOVERY

Accepted Article

Title: Discovery of Novel Biased Opioid Receptor Ligands through Structure-Based Pharmacophore Virtual Screening and Experiment

Authors: Pyeonghwa Jeong, Soo-Kyung Kim, Qianjie Li, Su-jin Oh, Seonil Son, Guangju Chen, Hongwei Tan, Siwon Kim, Jong-Hyun Park, Ki Duk Park, Yeo Ok Kim, Myung Ha Yoon, Yong-Chul Kim, and William Goddard III

This manuscript has been accepted after peer review and appears as an Accepted Article online prior to editing, proofing, and formal publication of the final Version of Record (VoR). This work is currently citable by using the Digital Object Identifier (DOI) given below. The VoR will be published online in Early View as soon as possible and may be different to this Accepted Article as a result of editing. Readers should obtain the VoR from the journal website shown below when it is published to ensure accuracy of information. The authors are responsible for the content of this Accepted Article.

To be cited as: *ChemMedChem* 10.1002/cmdc.201900418

Link to VoR: <http://dx.doi.org/10.1002/cmdc.201900418>

WILEY-VCH

www.chemmedchem.org

A Journal of



FULL PAPER

Discovery of Novel Biased Opioid Receptor Ligands through Structure-Based Pharmacophore Virtual Screening and Experiment

Pyeonghwa Jeong^{#,4}, Soo-Kyung Kim^{#,1}, Qianjie Li^{1,2,3}, Su-jin Oh⁵, Seonil Son⁵, Guangju Chen², Hongwei Tan², Siwon Kim^{6,7}, Jong-Hyun Park⁶, Ki Duk Park^{6,7,8}, Yeo Ok Kim⁹, Myung Ha Yoon⁹, Yong-Chul Kim^{4,5*}, William A. Goddard III^{1*}

[a] Prof. William A. Goddard III

¹Materials and Process Simulation Center (MC-139-74), California Institute of Technology, Pasadena, California 91125, US

E-mail: wag@caltech.edu ORCID:0000-0003-0097-5716;

Prof. Y.-C. Kim

⁵School of Life Sciences, ⁴Department of Biomedical Science & Engineering, Gwangju Institute of Science & Technology

123 Cheomdan-gwagi-ro, Buk-gu, 61005, South Korea

E-mail: yongchul@gist.ac.kr

[b] PH. Jeong

⁴Department of Biomedical Science & Engineering, Gwangju Institute of Science & Technology, 123 Cheomdan-gwagi-ro, Buk-gu, 61005, South Korea

Dr. S.-K. Kim

¹Materials and Process Simulation Center (MC-139-74), California Institute of Technology, Pasadena, California 91125, US

Dr. Q. Li

¹Material and Process Simulation Center (MC-139-14)

²College of Chemistry, Beijing Normal University

Beijing, 100875, People's Republic of China

³Institute of Medicinal Biotechnology, Chinese Academy of Medical Science, Beijing, 100050, People's Republic of China

S. Oh, S. Son

⁵School of Life Sciences, Gwangju Institute of Science & Technology

123 Cheomdan-gwagi-ro, Buk-gu, 61005, South Korea

Prof. G. Chen, Prof. H. Tan

²College of Chemistry, Beijing Normal University

Beijing, 100875, People's Republic of China

S. Kim

⁶Convergence Research Center for Diagnosis, Treatment and Care system of Dementia, Korea Institute of Science and Technology (KIST), Seoul 02792, South Korea

⁷Division of Bio-Medical Science & Technology, KIST School, Korea University of Science and Technology, Seoul 02792, South Korea

Dr. J.-H. Park

⁶Convergence Research Center for Diagnosis, Treatment and Care system of Dementia, Korea Institute of Science and Technology (KIST), Seoul 02792, South Korea

Dr. K.D. Park

⁶Convergence Research Center for Diagnosis, Treatment and Care system of Dementia, Korea Institute of Science and Technology (KIST), Seoul 02792, South Korea

⁷Division of Bio-Medical Science & Technology, KIST School, Korea University of Science and Technology, Seoul 02792, South Korea

⁸KHU-KIST Department of Converging Science and Technology, Kyung Hee University, Seoul 02447, South Korea

Prof. M.H. Yoon, Dr. Y.O. Kim

⁹Department of Anesthesiology and Pain Medicine, Medical School, Chonnam National University, Gwangju 501-757, South Korea

[#]These authors contributed equally to this work.

Abstract: G_i-protein biased agonists with minimal β-arrestin

recruitment have shown opportunities for alternative safe pain treatment to overcome the serious adverse effects of human mu opioid receptor (μ-OR) agonists. In order to discover novel non-morphine opioid receptor (OR) agonists, we applied hierarchical virtual screening of our in-house database against a pharmacophore based on modeling the active conformation of ORs. We discovered initial hit compound (**4**), a novel μ-OR agonist with pyrazoloisoquinoline scaffold. We applied computational R-group screening to compound **4** and synthesized 14 derivatives predicted to be best. Of these, the new G_i-protein biased compound (**19**) shows EC₅₀ = 179 nM at μ-OR. This resulting in significant pain-relief effects for mice at the phase II period in formalin tests. This study provides a new strategy to identify diverse sets of promising compounds that might prove useful for drug developments targeting other G protein-coupled receptors (GPCRs).

Introduction

Human mu opioid receptor (μ-OR) agonists such as morphine are clinically useful as effective analgesics for the treatment of moderate to severe pain.^[1] In addition, synthetic morphine (**1**, **Figure 1.**) analogues, e.g. buprenorphine^[2], and non-morphine synthetic compounds, e.g. fentanyl^[3], have been developed in recent decades to increase pharmacological activity and reduce side effects. Nevertheless, current treatment for pain using single administration of conventional opioids involves such risks as addiction, constipation, and respiratory depression^{[4],[5]}. Recent studies on biased G_i-protein activation with minimal β-arrestin recruitment showed opportunities for alternative efficient and more safe pain treatment to replace traditional narcotic analgesics.^[6] Accordingly, a G_i-biased μ-OR-specific agonist, TRV-130 (**2**, Oliceridine, **Figure 1.**),^[7] which showed significantly less side effects compared with morphine, has been developed and currently in the NDA stage of the US FDA^[8]. More recently, another biased agonist with highly selective pharmacological

FULL PAPER

profile to pain, PZM-21 (**3**, **Figure 1**).^[9] was discovered through structure based approaches using the antagonist bound μ -OR co-crystal structure for initial screening. However, recent studies have shown some controversial results of β -arrestin knock-out animal experiments, bringing forward a counterargument against the simple separation of therapeutic effects and side effects due to G_i -protein dependent signalling versus β -arrestin signalling.^[10] For example, although TRV-130 and PZM-21, the representative G_i -protein biased agonists, are devoid of addictive effects using conditioned place preference (CPP),^[9, 11] the research with β -arrestin knock-out mice showed enhanced morphine CPP, which provokes questions about the merits of G_i -protein biased opioid agonists. The controversial results might be explained by the lack of receptor desensitization of β -arrestin deficient conditions.^[12] Nevertheless, the discovery of novel G_i -protein biased μ -OR agonists and their precise pharmacological and preclinical studies are required for the development of safe opioid analgesics. Here, we report the discovery of non-morphine structural μ -OR agonists by means of additional refinements and optimization based on predicting the active G protein-coupled receptor (GPCR) conformations, *in-silico* screening, and side chain optimization. This led to the discovery of pyrazoloisoquinoline derivatives that provide a novel human μ -OR specific G_i -biased agonist chemotype, Compound 19, that leads to nanomolar EC_{50} values with minimal β -arrestin recruitment. The computational strategies used in this study should be useful for applications to other GPCRs.

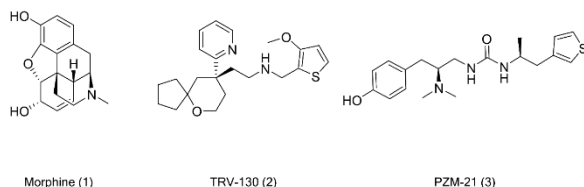


Figure 1. Structures of mu opioid receptor agonists.

Results and Discussion

Generating the ensemble of Opioid Receptors structures for ligand docking

In order to find optimum ligand-GPCR structures for novel ligands, we develop an ensemble of 25 GPCR conformations (with various tilts and rotations of the 7 transmembrane domains (TMD) expected to be thermally accessible. Here we use the GPCR Ensemble of Structures in Membrane BiLayer Environment (GEnSeMBLE) complete sampling method^[13], which has been applied successfully for adenosine A2A, Olfactory OR1G1, glucagon-like peptide GLP1, bitter taste TAS2R38, Chemokine CCR5, and cannabinoid CB1 receptors.^[14] Starting from templates having high homology to the μ -OR and κ -OR targets, we first fix the tilts and optimize simultaneous rotations about each of the 7 TMD. Considering rotation increments of 30° , we evaluate

the energy of all $(12)^7=35$ million packings in which the side chains are optimized independently for each pair of interacting TMDs (BiHelix). Then we select the top 1000, build the 7-TMD bundle, reassign side each of the side chains, evaluate the energy, and select 25 for further analysis (CombiHelix). We did this for 6 templates based on crystal structures of:

- μ -OR activated structures: BU72 agonist bound mouse μ -OR (PDB ID code 5C1M)^[15]
- κ -OR inactivated structures: antagonist JDtic bound to human κ -OR (PDB ID code 4DJH),^[16]
- Antagonist morphinan bonded to mouse μ -OR (PDB ID code 4DKL),^[17]
- Antagonist Naltrindole bonded to human δ -OR (PDB ID code 4N6H),^[18]
- Peptide mimetic antagonist compound-24 (C-24) bonded human nociceptin receptor (PDB ID code 4EA3),^[19] and
- One partial agonist (EKC) bonded to κ -OR.^[20]

From these $6*25 = 150$ packings, we selected the top 25 by energy and used the superfamily-wide GPCR Sequence-Structure (GRoSS) alignment of the TM for all 800 human GPCR sequences (based on maximizing the 8 inter-helical contacts characteristic of the activated GPCRs (the active hotspots) and 7 different contacts characteristic of inactive GPCRs (the GRoSS inactive hotspots). In the Top 25 of μ -OR structures from BiHelix, 13 structures are μ -OR templates (2 from inactive and 11 from active structures), 10 structures are from inactive δ -OR crystal structure, and 2 structures are from active κ -OR predicted model. These structures are tabulated in **Table S1** of the SI.

The next step in GEnSeMBLE is the SuperBiHelix optimization of tilts and rotations, allowing each tilt angle (θ) to change by 0 or $\pm 10^\circ$, each azimuthal projection (ϕ) to change by 0 or $\pm 15^\circ$, and each rotation (η) to change by 0 or $\pm 15^\circ$. We selected 3 following templates from BiHelix based on energy and diversity (see **Table S1** of the SI):

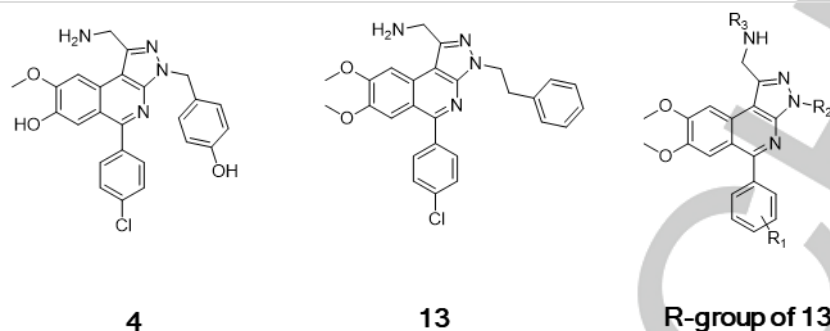
- the all-zero structure from the active μ -OR (BHtop1)
- the all-zero structure from the inactive δ -OR (BHtop2), and
- the all-zero structure from μ -OR (BHtop3).

For each of these 3, we optimized the side chains and predicted the energies for all $(3*5*5)^7 = 13$ trillion combinations of tilts and rotations. We selected the best 2000 to build the full 7-TMD bundle, repredicted the side chains and selected the best 25 by energy. From these 75 bundles we selected the best 25 based on energy for further analysis. Out of 25, 9 of the SuperBiHelix top25 (#2, 3, 4, 5, 8, 9, 10, 12,13) results are from the active crystal structure of μ -OR, the other 16 are from the inactive structure (**Table S2**).

The number of Class A conserved contacts, and the number and energy of interhelical hydrogen bonding are improved after SuperBiHelix sampling. The all-zero structure with the same rotation and tilting as the X-ray crystal structure of active μ -OR is ranked as topA8. The Active hotspot analysis using currently available X-ray of Class A GPCRs^[21] shows that some 10 of the top25 SuperBiHelix ensemble contain mainly active contacts (**Table S3**). The X-ray template of the active μ -OR bound to agonist has the most active hotspot contacts of 7, while the X-ray template of the inactive μ -OR bound to antagonist has the most inactive hot spot contacts of 7. The X-ray template for the inactive δ -OR and μ -OR has the most Class A contacts of 39. The highest hydrogen bond (HB) number increased through SuperBiHelix (20 to 27 for Inter HB, 39 to 46 for Tot HB). The best HB Energy was also improved (-55.25 to -62.43 for Inter HB E, -138.97 to -146.30

FULL PAPER

Table 1. Binding energy, % activation, and EC₅₀ of 14 compounds at 10 μM at hOPRM for Top 10 structures from the unified cavity energy (UCav) and the binding energy (BE) with ligand solvation (BE-Solv) rank from R-group screening. The table was ranked by % activation. The experiments show **19** to be the most active.



| Method | Compound | R1 | R2 | R3 | UCav ^[b] | BE-Solv ^[c] | % activation ^[d] | EC ₅₀ (nM) ^[d] |
|-------------------|-----------|--------------|--------------------------------------|----------|---------------------|------------------------|-----------------------------|--------------------------------------|
| VS ^[a] | 4 | | | | -35.87 | -55.44 | 50 ± 9.37 | 602 ± 33.35 |
| De novo | 13 | | | | -31.74 | -43.17 | 62.20 ± 11.81 | |
| UCav1 | 14 | <i>m</i> -Cl | <i>p</i> -NO ₂ -Bn | H | -43.57 | -38.70 | N.S ^[d] | |
| UCav2 | 15 | <i>m</i> -Cl | <i>m</i> -MeO-Bn | Dimethyl | -42.26 | -41.96 | 94.07 ± 1.33 | 235 ± 32.62 |
| UCav3 | 16 | <i>m</i> -Cl | naphthalen-2-ylmethyl | H | -42.17 | -38.54 | 46.07 ± 2.36 | |
| UCav4 | 17 | <i>o</i> -Cl | <i>m</i> -MeO-Bn | Dimethyl | -41.85 | -41.58 | N.S | |
| UCav5 | 18 | <i>p</i> -Cl | <i>m</i> -MeO-Bn | Dimethyl | -40.85 | -41.76 | N.S | |
| UCav6 | 19 | <i>m</i> -Cl | <i>p</i> -MeSO ₂ -Bn | Dimethyl | -40.61 | -41.36 | 100.01 ± 13.65 | 179 ± 21.83 |
| UCav7 | 20 | <i>m</i> -Cl | naphthalen-2-ylmethyl | Dimethyl | -40.07 | -40.47 | 64.95 ± 7.04 | |
| UCav8 | 21 | <i>o</i> -Cl | naphthalen-2-ylmethyl | H | -40.06 | -36.33 | N.S | |
| UCav9 | 22 | <i>p</i> -Cl | naphthalen-2-ylmethyl | H | -40.00 | -39.75 | 46.81 ± 6.18 | |
| UCav10 | 23 | <i>o</i> -Cl | naphthalen-2-ylmethyl | Dimethyl | -39.57 | -40.19 | N.S | |
| Method | Compound | R1 | R2 | R3 | UCav | BE-Solv | % activation | EC ₅₀ (nM) |
| BE-Solv1 | 24 | <i>m</i> -Cl | <i>p</i> -NO ₂ -phenethyl | Dimethyl | -52.08 | -39.31 | N.S | |
| BE-Solv2 | 25 | <i>m</i> -Cl | <i>p</i> -MeO- phenethyl | Dimethyl | -46.68 | -36.77 | 48.52 ± 0.14 | |
| BE-Solv3 | 26 | <i>p</i> -Cl | <i>p</i> -MeO- phenethyl | Dimethyl | -46.39 | -35.01 | 55.88 ± 5.92 | |
| BE-Solv4 | 27 | <i>o</i> -Cl | <i>p</i> -MeO- phenethyl | Dimethyl | -46.36 | -36.22 | 57.84 ± 10.82 | |
| BE-Solv5 | 28 | <i>o</i> -Cl | CH ₂ CH ₂ CN | Dimethyl | -46.00 | -34.17 | N.S | |
| BE-Solv6 | 29 | <i>m</i> -Cl | CH ₂ CH ₂ CN | Dimethyl | -45.94 | -34.04 | 87.00 ± 8.94 | 1,450 ± 360 |
| BE-Solv7 | 30 | <i>m</i> -Cl | isobutyl | Dimethyl | -45.94 | -28.16 | 44.11 ± 9.39 | |
| BE-Solv8 | 31 | <i>m</i> -Cl | 2-(N-methyl pyrrolidin-2-yl)ethyl | Dimethyl | -45.89 | -35.80 | 42.15 ± 6.07 | |
| BE-Solv9 | 32 | <i>m</i> -Cl | CH ₂ CH ₂ Cl | Dimethyl | -45.65 | -32.20 | N.S | |
| BE-Solv10 | 33 | <i>p</i> -Cl | isobutyl | Dimethyl | -45.58 | -26.56 | 79.17 ± 0.76 | 940 ± 43.37 |

[a] VS: Virtual screening, [b] UCav: unified cavity E is the nonbond energy between the ligand and the union of all protein residues within a constant cutoff distance of the ligand in all the complexes, [c] BE: vertical binding energy, snap binding E = complex E - protein E - ligand E. [d] All biological data were normalized compared to positive control DAMGO (3.7 μM) [e] N.S: not synthesized. All biological data were obtained by triplet testing and presented as the mean ± standard error of the mean (SEM).

for Sum HB E). The Class A contact number also increased from 39 to 40. Thus, the Top25 models exhibit a mixture of active and inactive ensembles. The predicted μ-OR structure exhibit the conserved TM hydrogen bond networks common to Class A GPCRs.^[22] The polar hydrogen bonding between L261 (5.65) backbone oxygen and R278 (6.31) is observed for 8 out of 25 structures. Consistent with traditional models of Class A GPCR activation, the active ensemble structures of μ-OR show TM5-6 interactions which are shown in Class A GPCRs. Using the same

methods, we predicted the ensemble of 25 structures for κ-OR (See Table S4-S5 in supporting information, SI).

Molecular Docking Studies

The in-house GIST database was developed to contain diverse heterocyclic core structures. To generate and visualize 3D conformers of molecules in the GIST data set, we used the design libraries tools in Discovery Studio 3.5. All generated ligands were energy minimized using the CHARMM (Chemistry at HARvard Macromolecular Mechanics) force field. These databases were

FULL PAPER

used for further structure-based virtual screening with our predicted active μ -OR conformation. To predict the optimum ligand binding site to each of the 25 protein conformations from the GEnSeMBLE procedure, we used the DarwinDock method to calculate the docking energy values of UCavE and SnapBE, which previously used to predict ligand-protein structures for

fluorescence-based assays (**Figure S1**). However, for κ -OR we observed no agonist activity ($\sim 1\%$ at $10 \mu\text{M}$) but good antagonist activity (84% at $30 \mu\text{M}$). The detailed synthetic procedures of compound **4** are described in the **Scheme S1**.

To understand the agonism of μ -OR and antagonism of κ -OR, we analysed the predicted binding pose of Compound **4**. (**Figure 2**) The common interactions are a salt bridge (SB) interactions from D3.32 residue. However, the orientation and the conformation of the ligands are different. The π - π interaction of **4** with the H6.52 residue in μ -OR is replaced with Y3.33 residue in κ -OR. There is an additional HB of the phenolic hydroxyl group to the unique W7.35 residue in μ -OR (Y7.35 residue in κ -OR or L7.35 residue in δ -OR). However, the K5.39 residue forms an HB with this hydroxyl group in κ -OR. Because of the different orientation, the A2.53 residue and Q2.60 residue interactions are observed only in μ -OR. Thus, various residues in the binding cavity and different conformations of μ -OR leads to a favourable binding pose for Compound **4**. Compound **4** in μ -OR prefers to bind to active structures #13 from SuperBihelix, while it binds to inactive structure #14 in κ -OR. Thus, these docking studies to subtypes of the OR explain fully why Compound **4** is an antagonist for κ -OR and an agonist for μ -OR. The best docking pose of μ -OR with **4** has UCavE of -35.87 and SnapBE of -69.76 kcal/mol. Compared to the inactive κ -OR (UCavE: -45.40 , SnapBE: -63.10 kcal/mol), μ -OR shows better SnapBE. In summary, Compound **4** prefers to bind to the active structure in μ -OR, while it binds to the inactive structure in κ -OR.

Summarizing, we discovered that compound **4** is a novel partial agonist for μ -OR and an antagonist for κ -OR. Next, we used *de novo* design with our predicted structure for compound **4** to simplify the synthetic process while increasing overall yield. We replaced the para-hydroxyl benzyl by a phenethyl group and we replaced the hydroxyl group at 7 position by a methoxy group in the isoquinoline ring. This modified compound **13** still shows 50% activation for μ -OR and 10% activation for κ -OR at $10 \mu\text{M}$ concentration (**Table 1**). **Fig. S2** shows the docking result of compound **13**. The common interactions are a SB interaction from D3.32 residue. There is an additional HB of the Nitrogen in the ring to Q2.60 residue in μ -OR. The π - π interaction of **13** was shown at the H6.52 residue in μ -OR.

To improve the activity and selectivity of compound **13**, we carried out R-group screening as follows:

- 1) At the R1 position (phenyl ring), we considered Cl at three positions: ortho, meta, and para)
- 2) At the R2 position, we considered 56 commercially available groups as summarized in **Figure S3**)
- 3) For the R3 position, we considered three cases: methyl and benzyl substitution or no substituent.

For lead optimization we calculated the binding energy for all $3 \times 56 \times 3 = 504$ cases to human μ -OR (topA-02). In each case we applied SCREAM (Side Chain Rotamer Excitation Analysis Method)^[23] to optimize the conformations for all residues in the binding site for all cases. The UCavE and the BE with solvation (BE-Solv) of the resulting ligand-protein complexes were calculated after 100 steps of energy minimization. Then we selected five compounds from the Top 10 of UCavE ranking and seven compounds from the Top 10 of BE-Solv ranking in the bold face in **Table 1**.

Chemistry

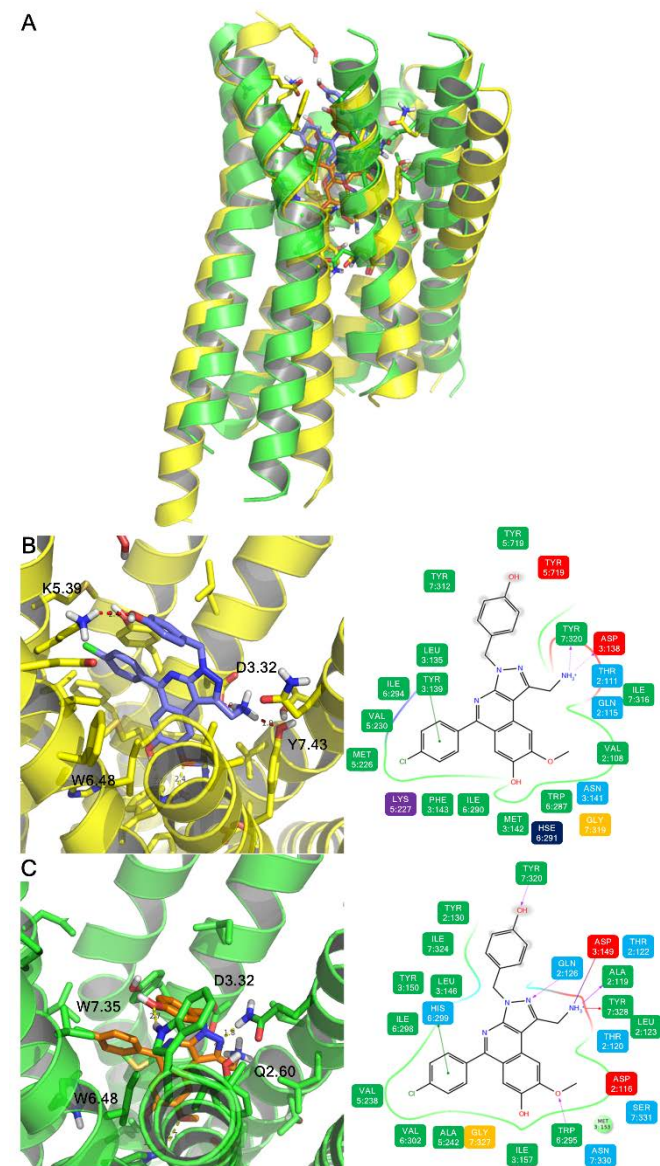
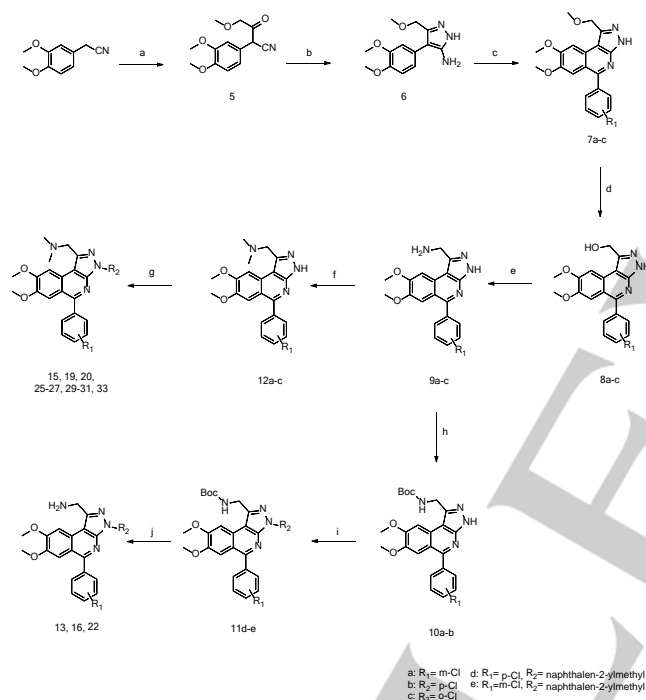


Figure 2. Predicted ligand-protein structures of compound **4** by molecular docking studies. (A) the superimposition of kappa (yellow) and mu (green) opioid receptor bound with compound **4**, (B) the binding site of kappa opioid receptor, and (C) the binding site of mu opioid receptor. The H-bond is represented by the arrows between the donor and the acceptor. Residues within 4 Å of ligand are shown on the corresponding 2D ligand interaction diagram displayed on the right. For clarity, only polar hydrogen atoms were shown. Here the color code is that dark blue is charged, light blue is polar amino acid, green is nonpolar hydrophobic amino acid, and orange is glycine.

many GPCRs.^[14] After this initial screening, we selected compound **4** to be synthesized. We used 12 steps overall with poor yield. We found that compound **4** showed 50% activation of μ -OR at $10 \mu\text{M}$ compared to the DAMGO positive control, using

FULL PAPER

Based on the predictions from computer-aided molecular design, we synthesized candidate compounds as shown in **Scheme 1** and **S1**. The detailed synthetic procedures of initial hit compound **4** and common intermediates **5** and **6** are described in **Scheme S1**. The synthesis of 13 derivatives selected from *de novo* design and R-group screening results at μ -OR is depicted in **Scheme 1**. Briefly, cyclization of the pyrazole intermediate, **6**, with various benzaldehydes using microwave irradiation gave **7a-c**. After O-demethylation using reactions using thionyl chloride and 2M ammonia solution in THF, respectively to provide **9a-c**. The final dimethyl amino derivatives, **15**, **19**, **20**, **25-27**, **29-31** and **33** were obtained by reductive amination reactions with formaldehyde (**12a-c**) and N-alkylations of pyrazole moieties with various R_2 groups. For the synthesis of final primary amine derivatives, **13**, **16** and **22**, the primary amines of **9a-c** were first protected with Boc group (**10a-b**), alkylation reactions (**11a-c**) and de-protection of the Boc group were accomplished.



Scheme 1. Reagents and conditions : (a) Ethyl methoxy acetate, potassium tert-butoxide, THF, rt, 2 h; (ii) Hydrazine hydrate, Acetic acid, MeOH, reflux, 4 h; (c) Various benzaldehyde, TFA, Microwave irradiation, 140°C, 2 h; (d) BBR_3 , DCM, 0°C, 4 h; (e) Thionyl chloride, reflux, 2 h then 2M NH_3 solution, THF 1 h; (f) 37% formaldehyde in water, sodium cyanoborohydride, acetic acid, DCE, rt, 3 h; (g) Cesium carbonate, various halide, DMF, rt; (h) Boc-anhydride, TEA, DCM, rt, 1 h; (i) 2-bromomethyl naphthalene, cesium carbonate, DMF, rt, 4 h; (j) TFA, DCM, 0°C, 1 h.

Biological Evaluation of Synthesized Compounds

The predicted compounds from R-group screening were tested for agonist activity using a calcium flux FLIPR assay. In this assay, all 14 synthesized compounds showed activation of human μ -OR signal at the concentration of 10 μM . (**Table 1** and **Figure 3A**). Particularly, compounds **15** and **19** promoted as much activity as DAMGO (94% and 100% of 3.7 μM DAMGO activity, respectively). The remaining 12 compounds showed partial agonism of μ -OR in calcium flux FLIPR assay. The four most effective compounds (**15**,

19, **29**, and **33**) were further tested for the concentration-dependency to calculate EC_{50} values (**Figure 3B**). Among them,

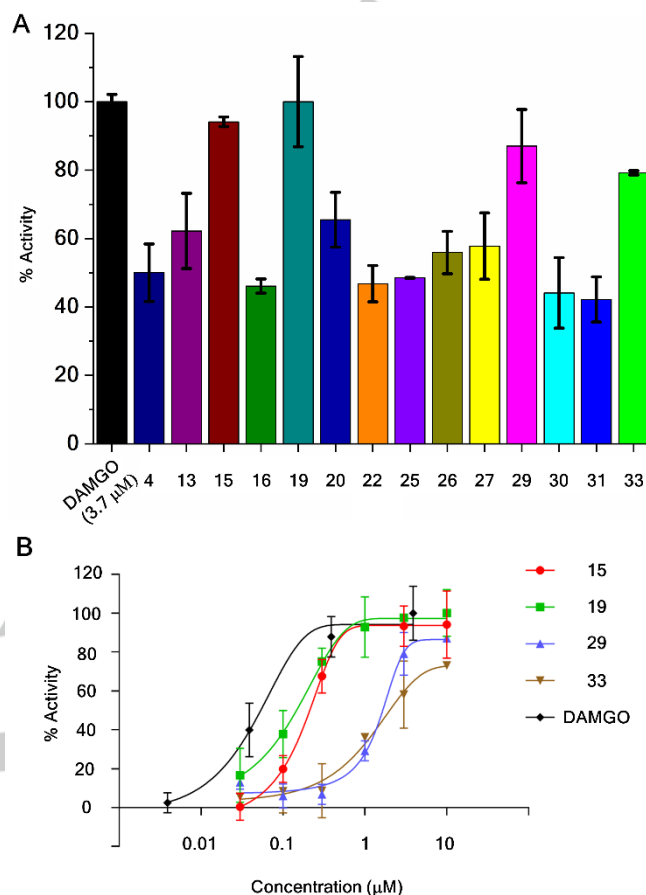


Figure 3. (A) Relative agonist activity of human μ opioid receptor (μ -OR) in calcium flux FLIPR assay at the concentration of 10 μM of compounds suggested by R-group screening, (B) The dose-response activation of the selected compounds at human μ -OR. Agonist activity was normalized to that of 3.7 μM DAMGO. All data were obtained by triplet testing and the error bars are the mean (SEM)

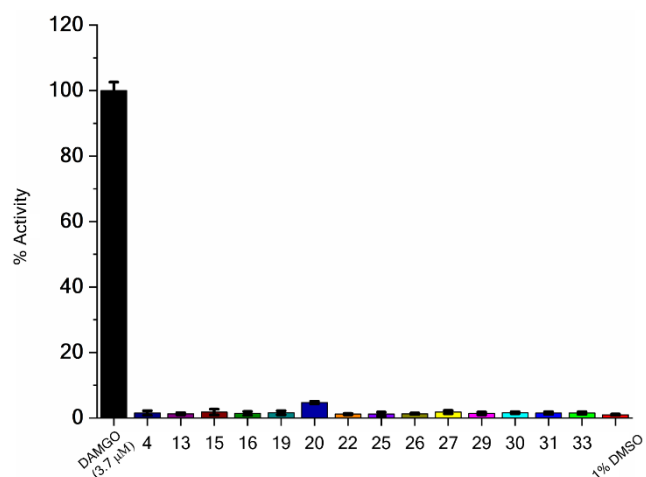


Figure 4. Agonist activity in β -arrestin recruitment assay at the concentration of 10 μM . Agonist activity was normalized to that of 3.7 μM of DAMGO. All data were obtained by triplet testing and the error bars are standard deviations.

FULL PAPER

Compound **19** displayed the best efficacy with an EC_{50} value of 179 nM. In addition, the best μ -OR agonists, Compound **15** and **19**, showed no κ -OR or δ -OR agonism (See Supporting information). All 14 compounds that displayed μ -OR agonism were tested at concentration of 10 μ M for β -arrestin recruitment assay. All 14 showed minimal β -arrestin recruitment compared to DAMGO (**Figure 4**). This result indicates that the new series of pyrazoloisoquinoline derivatives are G_i -biased agonists for μ -OR.

In Vivo Experiment of Compound 15 and 19

We investigated the in vivo analgesic effects of newly developed μ -OR biased agonists, compound **15** and **19**, for the initial proof of concept in formalin induced pain animal models. Subcutaneous injection of 50 μ L of 5% formalin solution was performed into the plantar surface of the hind paw to induce nociception 10 mins after pre-treatment with 10 μ g of compound **19** and 30 μ g of compound **15**, respectively. The morphine (3 μ g) was used as a positive control. The behavioural responses were measured by counting the number of rat flinches for 1 min periods from 1 to 2 min, 5 to 6 min and every 5 min from 10 to 60 min. Both compounds displayed significant analgesic effects at the phase II period of inflammatory pain with more than 80 % reduction (**Figure 5**).

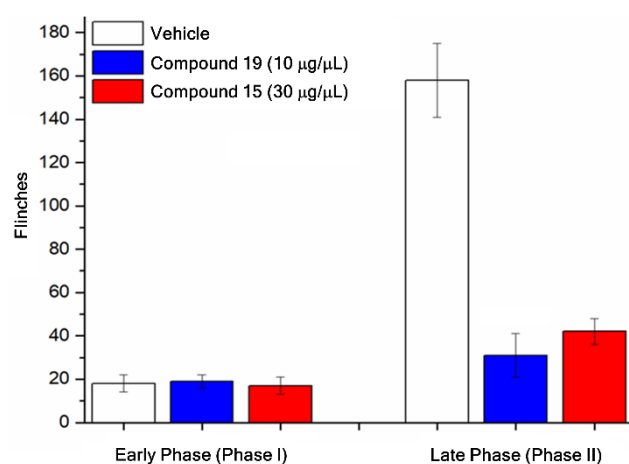


Figure 5. Reduced pain behavior in formalin injection test. Animals were pre-treated with vehicle (white, $n = 4$), compound **15** at 30 μ g/10 μ L (red, $n=4$) and **19** at 10 μ g/10 μ L (blue, $n=4$). Results are presented as the mean \pm standard error of the mean (SEM).

Binding Pose Analysis of Compound 19

Figure 6A and **B** shows the predicted binding pose of **19** in μ -OR. The major interactions are a SB between the protonated amine of the ligand and the D149 (3.32) residue. There is also a π - π interaction of the diphenyl ring of **19** with the Y150 (3.33) residue in μ -OR. However, the orientation of phenyl ring is different from compound **4**. The methane sulfonyl benzyl moiety of compound **19** is directed toward TM2 rather than TM7. Superimposing compound **19** into the binding site of the conventional μ -OR agonist, BU72, in green (**Figure 6C**) and the biased μ -OR agonist, PZM-21, in yellow (**Figure 6D**), we see that this methyl sulfoxide phenyl ring overlaps the thiophene ring of PZM-21 (**Figure 6D**). Based on the similarity to the PZM-21 binding site, we expected compound **19** to be a G_i -protein biased μ -OR agonist like PZM-21. Indeed, this was validated by the β -arrestin recruitment assay

in **Figure 4**. The additional binding site at the upper TM2 seems to be critical to exhibit G_i -protein biased agonism. This is plausible since binding or stabilizing the upper TM2 might affect the stability of TM1-2-7 network connecting to helix 8 and the C-terminal end that is an anchoring site of the β -arrestin.

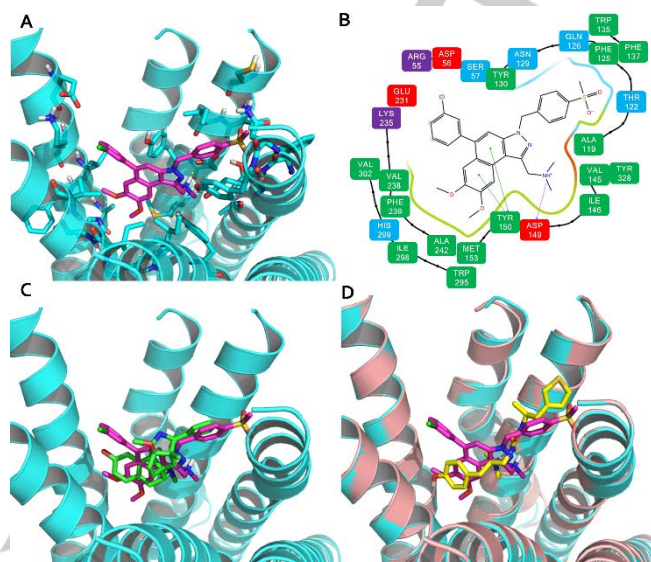


Figure 6. Binding site and comparisons of compound **19** with other μ -OR agonists. (A) the binding site for μ -OR, (B) 2D ligand interaction diagram, and superimposition with (C) the conventional μ -OR agonist, BU72, in green and (D) the biased μ -OR agonist, PZM-21, in yellow. The H-bond is represented by the arrows between the donor and the acceptor. Residues within 4 Å of ligand are shown on the 2D ligand interaction diagram displayed on the right. For clarity, only polar hydrogen atoms are shown.

Conclusions

In summary, we used ensemble docking based on the predicted ensemble of 25 predicted best GPCR packings (from GEnSeMBLE) to predict active conformation of μ -OR for *in silico* lead discovery. This was followed by experimental testing of the best cases to find new lead compound **4** with a novel pyrazoloquinoline scaffold exhibiting has $EC_{50} = 602$ nM with a maximum 50% activity for μ -OR. Then we applied R-group computational optimization with the predicted binding site for 504 combinations. This was followed by experimental screening of 14 cases to discover compound **19**: a fully active agonist with an EC_{50} of 179 nM at μ -OR and biased activity for all 14. This led to our discovery of the new pyrazolo[3,4-c]isoquinoline derivatives as G_i -protein biased full agonists at μ -OR, constituting new candidates for μ -OR pharmacology, distinct from such conventional nonbiased agonists as morphine. We further validated the *in vivo* analgesic effects of two new G_i -biased μ -OR agonists using the formalin induced nociception model studies in rats. We found significant analgesic effects of both compounds. This combined computational *in silico* optimization with experimental synthesis and characterization procedure successfully developed novel selective biased agonists for μ -OR provides an improved strategy to search for diverse new promising compounds. We expect that this procedure will be useful for other GPCR targeting drug developments.

FULL PAPER

Experimental Section

DarwinDock

For each of the 25 protein conformations and each of the 10-20 ligand conformations obtained for conformational search, we generated iteratively ~50,000 poses spanning the putative binding regions of the bulky residue-alarized protein. These poses were generated in increments of 5,000 and clustered into Voronoi families based on RMSD until <2% new families are generated. The family heads were scored using the Dreiding force field^[24] and the top10% by total energy were selected. Then we calculated the binding energy of all the members of these top 10% of families and selected the lowest 100 poses for further optimization. At this point the protein side chains were de-alarized using SCREAM^[23] to find the optimum side chains for each of the 100 poses. Then we neutralized the protein and the ligand by transferring protons appropriately within SB and protonating or deprotonating exterior ligands, followed by further full geometry minimization. The final docked structure with the best binding energy was selected.

Materials

Starting materials, reagents, and solvents were purchased from commercial suppliers and used as supplied without further purification. Thin layer chromatography (TLC) was performed on fluorescent silica gel plates (60 F253 from Merck) and visualized with either short wave ultra violet light at 254nm or 365nm. Microwave irradiation and conventional heating systems were achieved using Anton-paar Monowave 400 and Monowave 50, respectively. Chromatography purifications were achieved using kieselgel 60 (Merck) 0.040-0.0636 mm column chromatography. ¹H NMR was recorded on a JEOL JNM-ECX 400P spectrometer at 400 MHz and spectra were taken in CDCl₃ and DMSO-d₆. All NMR data were processed by ACD NMR Processor Academic version. Chemical shifts are expressed as ppm and coupling constants in Hz. Data were reported as follows: chemical shift, multiplicity (s, singlet; d, doublet; t, triplet; dd, doublet of doublet; ddd, doublet of doublet of doublet; m, multiplet), integration, and coupling constant.

4-(3,4-dimethoxyphenyl)-3-(methoxymethyl)-1H-pyrazol-5-amine (6)

The compound 5 (500 mg, 2 mmol) was fully dissolved in methanol with 3% acetic acid and then hydrazine hydrate (2 ml) was added dropwise with stirring. The reaction mixture was refluxed at 150°C for 4 h then cooled gradually to ambient temperature. The solvent was removed under reduced pressure and purified by silica gel column chromatography with MeOH:CHCl₃ (5%) to yield **6** as a yellow solid. ¹H NMR (400 MHz, CDCl₃) δ 6.96 (d, J=1.83Hz, 1 H), 6.95 - 6.92 (m, 1 H), 6.91 - 6.87 (m, 1 H), 4.45 (s, 2 H), 3.90 (s, 3 H), 3.91 (s, 3 H), 3.40 (s, 3 H).

General Procedure I for the preparation of compounds (7a-c)

To a microwave tube charged with chloro-substituted benzaldehyde (100 mg, 0.710 mmol) and compound **6** (150 mg, 0.592 mmol) in trifluoroacetic acid (2 ml) was added. The reaction was irradiated at 140°C for 2 h in the microwave apparatus, cooled to room temperature. The reaction mixture was concentrated in vacuo and dried to afford (**7a-c**) compound as a pale-yellow solid.

5-(3-chlorophenyl)-7,8-dimethoxy-1-(methoxymethyl)-3H-pyrazolo[3,4-c]isoquinoline (7a)

Compound **6** was reacted with 3-chlorobenzaldehyde according to the general procedure I, to yield the compound **7a** as a pale yellow solid. ¹H NMR (400 MHz, CDCl₃) δ 8.00 (s, 1 H), 7.75 - 7.73 (m, 1 H), 7.62 (ddd, J=6.30, 2.40, 1.60 Hz, 1 H), 7.54 - 7.50 (m, 2 H), 7.42 (s, 1 H), 5.04 (s, 2 H), 4.14 (s, 3 H), 3.87 (s, 3 H), 3.50 (s, 3 H).

5-(4-chlorophenyl)-7,8-dimethoxy-1-(methoxymethyl)-3H-pyrazolo[3,4-c]isoquinoline (7b)

Compound **6** was reacted with 4-chlorobenzaldehyde according to the general procedure I, to yield the compound **7b** as a pale yellow solid. ¹H NMR (400 MHz, CDCl₃) δ 8.00 (s, 1 H), 7.71 - 7.66 (m, 2 H), 7.58 - 7.53 (m, 2 H), 7.42 (s, 1 H), 5.03 (s, 2 H), 4.13 (s, 3 H), 3.87 (s, 3 H), 3.49 (s, 3 H).

5-(2-chlorophenyl)-7,8-dimethoxy-1-(methoxymethyl)-3H-pyrazolo[3,4-c]isoquinoline (7c)

Compound **6** was reacted with 2-chlorobenzaldehyde according to the general procedure I, to yield the compound **7c** as a pale yellow solid. ¹H NMR (400 MHz, CDCl₃) δ 8.00 (s, 1 H), 7.63 - 7.57 (m, 1 H), 7.55 - 7.45 (m, 3 H), 7.00 (s, 1 H), 5.05 (d, J=1.60 Hz, 2 H), 4.14 (s, 3 H), 3.81 (s, 3 H), 3.52 (s, 3 H).

General Procedure II for the preparation of compounds-demethylation

(5-(3-chlorophenyl)-7,8-dimethoxy-3H-pyrazolo[3,4-c]isoquinolin-1-yl)methanol (8a)

The compound **7a** (30 mg, 0.078 mmol) was dissolved in dichloromethane (3 mL) under argon atmosphere then 1 M boron tribromide in dichloromethane solution was added dropwise at 0 °C. The resulting mixture was kept in ice bath for 4 h and quenched with saturated aqueous ammonium chloride and extracted with dichloromethane 3 times. The organic layers were combined and dried with anhydrous Na₂SO₄. After Na₂SO₄ was removed, the organic layer was concentrated under reduced pressure and purified by silica gel column chromatography with MeOH:CHCl₃ (5%) to afford **8a** as a yellow solid. ¹H NMR (400 MHz, DMSO-d₆) δ 8.06 (s, 1 H), 7.80 - 7.74 (m, 2 H),

FULL PAPER

7.66 - 7.62 (m, 2 H), 7.37 (s, 1 H), 4.95 - 5.01 (m, 2 H), 4.01 (s, 3H), 3.75 (s, 3 H).

(5-(4-chlorophenyl)-7,8-dimethoxy-3H-pyrazolo[3,4-c]isoquinolin-1-yl)methanol (8b)

Followed by the procedure II, compounds **8b** were obtained from compounds **7b**. ¹H NMR (400 MHz, DMSO-*d*₆) δ 8.06 (s, 1 H), 7.80 - 7.74 (m, 2 H), 7.66 - 7.62 (m, 2 H), 7.37 (s, 1 H), 4.95 - 5.01 (m, 2 H), 4.01 (s, 3H), 3.75 (s, 3 H).

(5-(2-chlorophenyl)-7,8-dimethoxy-3H-pyrazolo[3,4-c]isoquinolin-1-yl)methanol (8c)

Followed by the procedure II, compounds **8c** were obtained from compounds **7c**. ¹H NMR (400 MHz, DMSO-*d*₆) δ 8.06 (s, 1 H), 7.71 - 7.66 (m, 1 H), 7.63 - 7.54 (m, 3 H), 6.83 (s, 1 H), 5.00 (br. s., 2 H), 4.01 (s, 3H), 3.63 (s, 3H).

General procedure III – amination followed by chlorination

(5-(3-chlorophenyl)-7,8-dimethoxy-3H-pyrazolo[3,4-c]isoquinolin-1-yl)methanamine (9a)

The compound **8a** (20 mg, 0.054 mmol) was added in SOCl₂ (2 mL) and refluxed at 80°C for 2 h. Excess SOCl₂ was removed under reduced pressure. The residual dark-brown crystalline was dissolved in 3 mL of tetrahydrofuran (THF), and 2 M ammonia solution in THF (1 mL) was added. After being stirred at room temperature for 1 h, the reaction mixture was diluted with ethyl acetate and quenched with aqueous 1N HCl. The organic layer was separated and washed with brine twice and dried with anhydrous Na₂SO₄. After Na₂SO₄ was filtered, solvent was removed in vacuum. The residue was purified by silica gel column chromatography with MeOH:CHCl₃ (2%) to afford **9a** as an off-white liquid. ¹H NMR (400 MHz, CDCl₃) δ 7.96 (s, 1 H), 7.75 - 7.73 (m, 1 H), 7.63 - 7.59 (m, 1 H), 7.56 - 7.50 (m, 2 H), 7.43 (s, 1 H), 5.27 (s, 2 H), 4.15 (s, 3 H), 3.88 (s, 3 H).

(5-(4-chlorophenyl)-7,8-dimethoxy-3H-pyrazolo[3,4-c]isoquinolin-1-yl)methanamine (9b)

Followed by the procedure III, compound **9b** was obtained from compound **8b**. ¹H NMR (400 MHz, DMSO-*d*₆) δ 8.08 (s, 1 H), 7.81 - 7.73 (m, 2 H), 7.68 - 7.61 (m, 2 H), 7.37 (s, 1 H), 4.33 (s, 2 H), 4.04 (s, 3 H), 3.76 (s, 3 H).

(5-(2-chlorophenyl)-7,8-dimethoxy-3H-pyrazolo[3,4-c]isoquinolin-1-yl)methanamine (9c)

Followed by the procedure III, compound **9c** was obtained from compound **8c**. ¹H NMR (400 MHz, CDCl₃) δ 7.84 (s, 1 H), 7.42 - 7.64 (m, 4 H), 6.98 (s, 1 H), 4.56 (s, 2 H), 4.13 (s, 3 H), 3.79 (s, 3 H).

tert-butyl ((5-(3-chlorophenyl)-7,8-dimethoxy-3H-pyrazolo[3,4-c]isoquinolin-1-yl)methyl)carbamate (10a)

To a solution of compound **9a** (90 mg, 0.244 mmol) in dichloromethane (5 mL) was treated with di-*tert*-butyl dicarbonate (106 mg, 0.488 mmol) and triethylamine (49 mg, 0.488 mmol). The reaction mixture was stirred at room temperature for 1 h. After the reaction was completed, the residue was diluted with saturated aqueous ammonium chloride and extracted with dichloromethane 3 times. The organic layer was dried over anhydrous MgSO₄, filtered and concentrated under reduced pressure. The crude materials were treated with diethyl ether and the mixture was filtrated to obtain compound **10a** as a pale-yellow solid. ¹H NMR (400 MHz, DMSO-*d*₆) δ 7.92 - 7.86 (m, 2 H), 7.82 - 7.75 (m, 2 H), 7.73 - 7.68 (m, 1 H), 7.67 - 7.59 (m, 2 H), 4.83 - 4.70 (m, 2 H), 4.06 (s, 3 H), 3.75 (s, 3H), 1.43 - 1.38 (m, 9 H).

tert-butyl ((5-(4-chlorophenyl)-7,8-dimethoxy-3H-pyrazolo[3,4-c]isoquinolin-1-yl)methyl)carbamate (10b)

To a solution of compound **9b** (90 mg, 0.244 mmol) in dichloromethane (5 mL) was treated with di-*tert*-butyl dicarbonate (106 mg, 0.488 mmol) and triethylamine (49 mg, 0.488 mmol). The reaction mixture was stirred at room temperature for 1 h. After the reaction was completed, the residue was diluted with saturated aqueous ammonium chloride and extracted with dichloromethane 3 times. The organic layer was dried over anhydrous MgSO₄, filtered and concentrated under reduced pressure. The crude materials were treated with diethyl ether and the mixture was filtrated to obtain compound **10b** as a pale-yellow solid. ¹H NMR (400 MHz, CDCl₃) δ 7.76 (s, 1 H), 7.72 - 7.63 (m, 2 H), 7.60 - 7.52 (m, 2 H), 7.41 (s, 1H), 5.06 - 4.95 (m, 2 H), 4.17 (s, 3 H), 3.85 (s, 3 H), 1.52 - 1.46 (m, 9 H).

tert-butyl ((5-(2-chlorophenyl)-7,8-dimethoxy-3H-pyrazolo[3,4-c]isoquinolin-1-yl)methyl)carbamate (10c)

To a solution of compound **9c** (90 mg, 0.244 mmol) in dichloromethane (5 mL) was treated with di-*tert*-butyl dicarbonate (106 mg, 0.488 mmol) and triethylamine (49 mg, 0.488 mmol). The reaction mixture was stirred at room temperature for 1 h. After the reaction was completed, the residue was diluted with saturated aqueous ammonium chloride and extracted with dichloromethane 3 times. The organic layer was dried over anhydrous MgSO₄, filtered and concentrated under reduced pressure. The crude materials were treated with diethyl ether and the mixture was filtrated to obtain compound **10c** as a white solid. ¹H NMR (400 MHz, CDCl₃) δ 7.78 (s, 1 H), 7.62 - 7.57 (m, 1 H), 7.53 - 7.45 (m, 3 H), 7.00 (s, 1 H), 5.04 - 4.95 (m, 2 H), 4.17 (s, 3 H), 3.80 (s, 3H), 1.53 - 1.45 (m, 9 H).

FULL PAPER

Tert-butyl ((5-(3-chlorophenyl)-7,8-dimethoxy-3-(naphthalen-2-ylmethyl)-3H-pyrazolo[3,4-c]isoquinolin-1-yl)methyl)carbamate (11d)

To a solution of compound **10b** (40 mg, 0.085 mmol) in dried DMF in the presence of cesium carbonate (55 mg, 0.170 mmol) was added 2-(bromomethyl)naphthalene (37.5 mg, 0.170 mmol). After the mixture was stirred at room temperature for 3 h, the solvent was removed in vacuo. The residue was taken up in solution of saturated aqueous ammonium chloride and extracted with ethyl acetate twice. The combined extract was dried with anhydrous Na₂SO₄, filtered and evaporated. The residue was purified by silica gel column chromatography with MeOH:CHCl₃ (1%) to afford **11d** as a pale-yellow oily liquid. ¹H NMR (400 MHz, CDCl₃) δ 7.87 - 7.73 (m, 6 H), 7.64 - 7.61 (m, 1 H), 7.53 - 7.41 (m, 6 H), 5.89 (s, 2 H), 5.10 (br. s., 1 H), 4.95 (d, J=5.50 Hz, 2 H), 4.15 (s, 3 H), 3.86 (s, 3 H), 1.45 (s, 9 H).

Tert-butyl ((5-(4-chlorophenyl)-7,8-dimethoxy-3-(naphthalen-2-ylmethyl)-3H-pyrazolo[3,4-c]isoquinolin-1-yl)methyl)carbamate (11e)

To a solution of compound **10a** (40 mg, 0.085 mmol) in dried DMF in the presence of cesium carbonate (55 mg, 0.170 mmol) was added 2-(bromomethyl)naphthalene (37.5 mg, 0.170 mmol). After the mixture was stirred at room temperature for 4 h, the solvent was removed in vacuo. The residue was taken up in solution of saturated aqueous ammonium chloride and extracted with ethyl acetate twice. The combined extract was dried with anhydrous Na₂SO₄, filtered and evaporated. The residue was purified by silica gel column chromatography with MeOH:CHCl₃ (1%) to afford compound **11e** as a transparent liquid. ¹H NMR (400 MHz, CDCl₃) δ 7.81 - 7.74 (m, 5 H), 7.73 - 7.67 (m, 2 H), 7.58 - 7.52 (m, 2 H), 7.49 - 7.42 (m, 4 H), 5.88 (s, 2 H), 5.11 (br. s., 1 H), 4.94 (d, J=5.50 Hz, 2 H), 4.16 (s, 3 H), 3.86 (s, 3 H), 1.45 (s, 9 H).

General procedure IV – reductive amination**1-(5-(3-chlorophenyl)-7,8-dimethoxy-3H-pyrazolo[3,4-c]isoquinolin-1-yl)-N,N-dimethylmethanamine (12a)**

To a solution of compound **9a** (200 mg, 0.54 mmol) in 1,2-dichloroethane with 5% acetic acid, sodium cyanoborohydride (340 mg, 1.62 mmol) was added followed by 37% formaldehyde in water (300 μL, 3.8 mmol) and stirred at room temperature for 3 h. The crude reaction mixture was quenched with saturated aqueous sodium bicarbonate and extracted with dichloromethane twice. The combined organic layer as dried with anhydrous Na₂SO₄. After Na₂SO₄ was filtered, solvent was removed in vacuum. The residue was purified by silica gel column chromatography with MeOH:CHCl₃ (2%) to give **12a** as a colourless liquid. ¹H NMR (400 MHz, CDCl₃) δ 8.43 (s, 1 H), 7.76 - 7.73 (m, 1 H), 7.64 - 7.59 (m, 1 H), 7.55 - 7.48 (m, 2 H), 7.41 (s, 1 H), 4.15 (s, 3 H), 3.98 (s, 2 H), 3.88 (s, 3 H), 2.42 (s, 6 H).

1-(5-(4-chlorophenyl)-7,8-dimethoxy-3H-pyrazolo[3,4-c]isoquinolin-1-yl)-N,N-dimethylmethanamine (12b)

Following the general procedure IV, compound **12b** was obtained from compound **8b**. ¹H NMR (400 MHz, CDCl₃) δ 8.43 (s, 1 H), 7.73 - 7.67 (m, 2 H), 7.59 - 7.53 (m, 2 H), 7.41 (s, 1 H), 4.15 (s, 3 H), 3.99 (s, 2 H), 3.87 (s, 3 H), 2.42 (s, 6 H).

1-(5-(2-chlorophenyl)-7,8-dimethoxy-3H-pyrazolo[3,4-c]isoquinolin-1-yl)-N,N-dimethylmethanamine (12c)

Following the general procedure IV, compound **12c** was obtained from compound **8c**. ¹H NMR (400 MHz, CDCl₃) δ 8.40 (s, 1 H), 7.57 - 7.61 (m, 1 H), 7.46 - 7.53 (m, 3 H), 6.98 (s, 1 H), 4.14 (s, 3 H), 3.99 (d, J=4.27 Hz, 2 H), 3.80 (s, 3 H), 2.43 (s, 6 H).

(5-(4-chlorophenyl)-7,8-dimethoxy-3-phenethyl-3H-pyrazolo[3,4-c]isoquinolin-1-yl)methanamine (13)

A solution of compound **11c** (17 mg, 0.029 mmol) in dichloromethane (5 mL) was cooled to 0°C, and trifluoroacetic acid (1 mL) was slowly added. Upon completion of reaction, the mixture was concentrated under reduced pressure. The residue was taken up in solution of saturated aqueous sodium bicarbonate and extracted dichloromethane 3 times. The combined organic layer was dried with anhydrous Na₂SO₄. After Na₂SO₄ was filtered, solvent was removed in vacuum. The residue was purified by silica gel column chromatography with MeOH: ammonia saturated CHCl₃ (1%) to afford **13** as a brown liquid. ¹H NMR (400 MHz, MeOH-d₄) δ 7.66 (s, 1 H), 7.55 - 7.58 (m, 4 H), 7.33 (s, 1 H), 7.03 - 7.13 (m, 5 H), 4.72 - 4.77 (m, 2 H), 4.44 (m, 2 H), 4.08 (s, 3 H), 3.76 (s, 3 H), 3.20 (t, J=7.02 Hz, 2 H)

1-(5-(3-chlorophenyl)-7,8-dimethoxy-3-(3-methoxybenzyl)-3H-pyrazolo[3,4-c]isoquinolin-1-yl)-N,N-dimethylmethanamine (15)

To a solution of compound **12a** (40 mg, 0.085 mmol) in dried DMF in the presence of cesium carbonate (55 mg, 0.170 mmol) was added 3-methoxybenzyl bromide (26.2 mg, 0.130 mmol). After the mixture was stirred at room temperature for 1.5 h, the solvent was removed in vacuo. The residue was taken up in solution of saturated aqueous ammonium chloride and extracted with ethyl acetate twice. The combined extract was dried with anhydrous Na₂SO₄, filtered and evaporated. The residue was purified by silica gel column chromatography with MeOH:CHCl₃ (1%) to afford compound **15** as a white liquid (yield = 81%). ¹H NMR (500 MHz, CDCl₃) δ ppm 8.38 (s, 1 H), 7.74 - 7.76 (m, 1 H), 7.62 (ddd, J=6.42, 2.26, 1.59 Hz, 1 H), 7.49 - 7.51 (m, 2 H), 7.41 (s, 1 H), 7.20 (t, J=8.07 Hz, 1 H), 6.90 6.92 (m, 2 H), 6.77 - 6.79 (m, 1 H), 5.75 (s, 2 H), 4.13 (s, 4 H), 3.96 (s, 2 H), 3.87 (s, 3 H), 3.74 (s, 3 H), 2.40 (s, 6 H). ¹³C NMR (126 MHz, CDCl₃) δ ppm 157.87 (s, 1 C), 157.45 (s, 1 C), 153.63 (s, 1 C), 147.82 (s, 1 C), 143.25 (s, 1 C), 141.77 (s, 1 C), 139.09 (s, 1 C), 138.73 (s, 1 C), 134.50 (s, 1 C), 130.06 (s, 1 C), 129.58 (s, 1 C), 129.52 (s, 1 C), 129.46 (s, 1 C), 128.92 (s, 1 C), 128.78 (s, 1 C), 128.46 (s, 1 C), 128.03 (s, 1 C), 120.06 (s, 1 C), 113.72 (s, 1 C), 113.20 (s, 1 C), 105.49 (s, 1 C), 104.00 (s, 1 C), 56.18 (s, 1 C), 55.92 (s, 1 C), 55.92 (s, 1 C), 49.90 (s, 1 C), 44.53 (s, 1 C), 44.53 (s, 1 C), 40.99 (s, 1 C).

FULL PAPER

(5-(3-chlorophenyl)-7,8-dimethoxy-3-(naphthalen-2-ylmethyl)-3H-pyrazolo[3,4-c]isoquinolin-1-yl)methanamine (16)

A solution of compound **11b** (20 mg, 0.035 mmol) in dichloromethane (5 mL) was cooled to 0°C, and trifluoroacetic acid (1 mL) was slowly added. Upon completion of reaction, the mixture was concentrated under reduced pressure. The residue was taken up in solution of saturated aqueous sodium bicarbonate and extracted dichloromethane 3 times. The combined organic layer was dried with anhydrous Na₂SO₄. After Na₂SO₄ was filtered, solvent was removed in vacuum. The residue was purified by silica gel column chromatography with MeOH: ammonia saturated CHCl₃ (2%) to afford compound **16** as a yellow liquid. ¹H NMR (400 MHz, CDCl₃) δ 7.71 (s, 1 H), 7.61 - 7.35 (m, 9 H), 7.15 - 7.04 (m, 2 H), 6.91 - 6.78 (m, 1 H), 5.81 (s, 2 H), 4.47 (s, 2 H), 3.97 (s, 3 H), 3.86 (s, 3 H). ¹³C NMR (126 MHz, CDCl₃) δ ppm 157.67 (s, 1 C), 153.53 (s, 1 C), 147.84 (s, 1 C), 147.59 (s, 1 C), 145.15 (s, 1 C), 141.86 (s, 1 C), 134.89 (s, 1 C), 134.50 (s, 1 C), 133.29 (s, 1 C), 132.81 (s, 1 C), 130.10 (s, 1 C), 129.59 (s, 1 C), 128.88 (s, 1 C), 128.67 (s, 1 C), 128.28 (s, 1 C), 128.06 (s, 1 C), 127.92 (s, 1 C), 127.62 (s, 1 C), 126.91 (s, 1 C), 126.10 (s, 1 C), 125.99 (s, 1 C), 125.88 (s, 1 C), 118.29 (s, 1 C), 108.28 (s, 1 C), 106.64 (s, 1 C), 103.71 (s, 1 C), 77.22 (s, 1 C), 56.17 (s, 1 C), 55.92 (s, 1 C), 50.80 (s, 1 C), 41.33 (s, 1 C).

1-(5-(3-chlorophenyl)-7,8-dimethoxy-3-(4-(methylsulfonyl)benzyl)-3H-pyrazolo[3,4-c]isoquinolin-1-yl)-N,N-dimethylmethanamine (19)

To a solution of compound **12a** (40 mg, 0.085 mmol) in dried DMF in the presence of cesium carbonate (55 mg, 0.170 mmol) was added 4-(methylsulfonyl)benzyl bromide (37.1 mg, 0.140 mmol). After the mixture was stirred at room temperature for 1.5 h, the solvent was removed in vacuo. The residue was taken up in solution of saturated aqueous ammonium chloride and extracted with ethyl acetate twice. The combined extract was dried with anhydrous Na₂SO₄, filtered and evaporated. The residue was purified by silica gel column chromatography with MeOH:CHCl₃ (1%) to afford compound **19** as a white liquid (yield = 73%) ¹H NMR (400 MHz, CDCl₃-d) δ ppm 8.37 (s, 1 H), 7.83 - 7.86 (m, 2 H), 7.69 (dt, J=1.95, 1.09 Hz, 1 H), 7.58 (ddd, J=6.30, 2.40, 1.60 Hz, 1 H), 7.47 - 7.51 (m, 2 H), 7.42 - 7.46 (m, 2 H), 7.39 (s, 1 H), 5.84 (s, 2 H), 4.12 (s, 3 H), 3.94 (s, 2 H), 3.85 (s, 3 H), 2.99 (s, 3 H), 2.38 (s, 6 H). ¹³C NMR (126 MHz, CDCl₃) δ ppm 157.99 (s, 1 C), 153.54 (s, 1 C), 147.92 (s, 1 C), 147.82 (s, 1 C), 143.76 (s, 1 C), 143.68 (s, 1 C), 141.68 (s, 1 C), 139.63 (s, 1 C), 134.51 (s, 1 C), 129.96 (s, 1 C), 129.96 (s, 1 C), 129.63 (s, 1 C), 129.63 (s, 1 C), 128.97 (s, 1 C), 128.46 (s, 1 C), 128.46 (s, 1 C), 127.96 (s, 1 C), 127.70 (s, 1 C), 118.56 (s, 1 C), 108.12 (s, 1 C), 107.94 (s, 1 C), 56.18 (s, 1 C), 55.92 (s, 1 C), 55.92 (s, 1 C), 49.90 (s, 1 C), 44.53 (s, 1 C), 44.53 (s, 1 C), 40.99 (s, 1 C).

1-(5-(3-chlorophenyl)-7,8-dimethoxy-3-(naphthalen-2-ylmethyl)-3H-pyrazolo[3,4-c]isoquinolin-1-yl)-N,N-dimethylmethanamine (20)

To a solution of compound **12a** (40 mg, 0.1 mmol) in dried DMF in the presence of cesium carbonate (55 mg, 0.170 mmol) was added 2-bromomethyl naphthalene (37.6 mg, 0.17 mmol). After the mixture was stirred at room temperature for 2 h, the solvent was removed in vacuo.

The residue was taken up in solution of saturated aqueous ammonium chloride and extracted with ethyl acetate twice. The combined extract was dried with anhydrous Na₂SO₄, filtered and evaporated. The residue was purified by silica gel column chromatography with MeOH:CHCl₃ (1%) to afford compound **20** as a pale-yellow liquid. ¹H NMR (400 MHz, CDCl₃) δ 8.37 (s, 1 H), 7.82 - 7.72 (m, 5 H), 7.65 - 7.60 (m, 1 H), 7.53 - 7.40 (m, 6 H), 5.93 (s, 2 H), 4.13 (s, 3 H), 3.96 (s, 2 H), 3.86 (s, 3 H), 2.40 (s, 6 H). ¹³C NMR (126 MHz, CDCl₃) δ ppm 153.29 (s, 1 C), 147.89 (s, 1 C), 147.57 (s, 1 C), 141.95 (s, 1 C), 135.02 (s, 1 C), 134.46 (s, 1 C), 133.30 (s, 1 C), 132.77 (s, 1 C), 131.94 (s, 1 C), 131.12 (s, 1 C), 130.10 (s, 1 C), 129.59 (s, 1 C), 129.59 (s, 1 C), 128.81 (s, 1 C), 128.21 (s, 1 C), 128.06 (s, 1 C), 127.90 (s, 1 C), 127.90 (s, 1 C), 127.60 (s, 1 C), 126.70 (s, 1 C), 126.05 (s, 1 C), 125.82 (s, 1 C), 124.85 (s, 1 C), 118.36 (s, 1 C), 108.02 (s, 1 C), 107.88 (s, 1 C), 56.07 (s, 1 C), 55.90 (s, 1 C), 55.90 (s, 1 C), 50.78 (s, 1 C), 45.33 (s, 1 C), 45.33 (s, 1 C).

1-(5-(4-chlorophenyl)-7,8-dimethoxy-3-(naphthalen-2-ylmethyl)-3H-pyrazolo[3,4-c]isoquinolin-1-yl)methanamine (22)

A solution of compound **11a** (20 mg, 0.035 mmol) in dichloromethane (5 mL) was cooled to 0°C, and trifluoro acetic acid (1 mL) was slowly added. Upon completion of reaction, the mixture was concentrated under reduced pressure. The residue was taken up in solution of saturated aqueous sodium bicarbonate and extracted dichloromethane 3 times. The combined organic layer was dried with anhydrous Na₂SO₄. After Na₂SO₄ was filtered, solvent was removed in vacuum. The residue was purified by silica gel column chromatography with MeOH: ammonia saturated CHCl₃ (2%) to afford compound **22** as a brown liquid. ¹H NMR (400 MHz, CDCl₃) δ 7.67 - 7.62 (m, 2 H), 7.59 - 7.51 (m, 3 H), 7.48 - 7.41 (m, 2 H), 7.41 - 7.35 (m, 2 H), 7.14 - 7.05 (m, 2 H), 6.83 (br. s., 1 H), 5.81 (s, 2 H), 4.45 (br. s., 2H), 3.99 (s, 3 H) 3.86 (s, 3 H). ¹³C NMR (126 MHz, CDCl₃) δ ppm 157.05 (s, 1 C), 153.49 (s, 1 C), 147.90 (s, 1 C), 147.56 (s, 1 C), 145.19 (s, 1 C), 138.58 (s, 1 C), 134.96 (s, 1 C), 134.92 (s, 1 C), 133.29 (s, 1 C), 132.80 (s, 1 C), 131.26 (s, 1 C), 131.26 (s, 1 C), 128.67 (s, 1 C), 128.67 (s, 1 C), 128.27 (s, 1 C), 127.88 (s, 1 C), 127.88 (s, 1 C), 127.63 (s, 1 C), 126.82 (s, 1 C), 126.09 (s, 1 C), 125.94 (s, 1 C), 125.87 (s, 1 C), 118.33 (s, 1 C), 108.34 (s, 1 C), 106.54 (s, 1 C), 103.72 (s, 1 C), 56.17 (s, 1 C), 55.92 (s, 1 C), 50.80 (s, 1 C), 41.33 (s, 1 C).

1-(5-(3-chlorophenyl)-7,8-dimethoxy-3-(4-methoxyphenethyl)-3H-pyrazolo[3,4-c]isoquinolin-1-yl)-N,N-dimethylmethanamine (25)

To a solution of compound **12a** (40 mg, 0.1 mmol) in dried DMF in the presence of cesium carbonate (55 mg, 0.170 mmol) was added 4-(2-chloroethyl)anisole (14.5 mg, 0.170 mmol). After the mixture was stirred at room temperature for 1 h, the solvent was removed in vacuo. The residue was taken up in solution of saturated aqueous ammonium chloride and extracted with ethyl acetate twice. The combined extract was dried with anhydrous Na₂SO₄, filtered and evaporated. The residue was purified by silica gel column chromatography with MeOH:CHCl₃ (1%) to afford compound **25** as a pale-brown liquid. ¹H NMR (500 MHz, DMSO-d₆) δ ppm 8.20 (s, 1 H), 7.57 - 7.65 (m, 4 H), 7.29 (s, 1 H), 6.96 (m, J=8.80 Hz, 2 H), 6.68 (m, J=8.80 Hz, 2 H), 4.65 (t, J=6.97 Hz, 2 H), 4.01 (s, 3 H), 3.86 (s, 2 H), 3.72 (s, 3 H), 3.62 (s, 3 H), 3.12 (t, J=6.97 Hz, 2 H), 2.27 (s, 6 H). ¹³C NMR (126 MHz, DMSO-d₆) δ ppm 158.18 (s, 1 C), 156.55 (s, 1 C), 153.39 (s, 1 C), 147.70 (s, 1 C), 147.52 (s, 1 C), 142.16

FULL PAPER

(s, 1 C), 142.08 (s, 1 C), 133.71 (s, 1 C), 133.92 (s, 1 C), 130.84 (s, 1 C), 130.59 (s, 1 C), 130.16 (s, 1 C), 129.83 (s, 1 C), 129.09 (s, 1 C), 128.81 (s, 1 C), 128.42 (s, 1 C), 117.58 (s, 1 C), 114.29 (s, 1 C), 113.94 (s, 1 C), 107.85 (s, 1 C), 107.32 (s, 1 C), 105.88 (s, 1 C), 56.04 (s, 1 C), 55.89 (s, 1 C), 55.19 (s, 1 C), 55.19 (s, 1 C), 48.50 (s, 1 C), 45.26 (s, 1 C), 45.26 (s, 1 C), 35.50 (s, 1 C).

1-(5-(4-chlorophenyl)-3-isobutyl-7,8-dimethoxy-3H-pyrazolo[3,4-c]isoquinolin-1-yl)-N,N-dimethylmethanamine (26)

To a solution of compound **12b** (40 mg, 0.1 mmol) in dried DMF in the presence of cesium carbonate (55 mg, 0.170 mmol) was added 4-(2-chloroethyl)anisole (14.5 mg, 0.170 mmol). After the mixture was stirred at room temperature for 1 h, the solvent was removed in vacuo. The residue was taken up in solution of saturated aqueous ammonium chloride and extracted with ethyl acetate twice. The combined extract was dried with anhydrous Na₂SO₄, filtered and evaporated. The residue was purified by silica gel column chromatography with MeOH:CHCl₃ (1%) to afford compound **26** as a pale-brown liquid. ¹H NMR (400 MHz, CDCl₃) δ 8.34 (br. s., 1 H), 7.62 (m, J=8.56 Hz, 2 H), 7.53 (m, J=8.31 Hz, 2 H), 7.37 (s, 1 H), 7.09 - 7.03 (m, 2 H), 6.76 - 6.71 (m, 2 H), 4.76 (br. s., 2 H), 4.17 - 4.09 (s, 3H), 3.95 (br. s., 2 H), 3.85 (s, 3 H), 3.73 (s, 3 H), 3.22 (t, J=6.85 Hz, 2 H), 2.39 (br. s., 6 H). ¹³C NMR (126 MHz, CDCl₃) δ ppm 158.10 (s, 1 C), 153.13 (s, 1 C), 147.67 (s, 1 C), 147.42 (s, 1 C), 138.71 (s, 1 C), 134.75 (s, 1 C), 131.19 (s, 1 C), 131.19 (s, 1 C), 131.19 (s, 1 C), 130.65 (s, 1 C), 129.89 (s, 1 C), 129.89 (s, 1 C), 129.89 (s, 1 C), 128.57 (s, 1 C), 128.57 (s, 1 C), 128.57 (s, 1 C), 118.20 (s, 1 C), 113.71 (s, 1 C), 113.71 (s, 1 C), 113.71 (s, 1 C), 107.95 (s, 1 C), 103.62 (s, 1 C), 56.04 (s, 1 C), 55.89 (s, 1 C), 55.19 (s, 1 C), 55.19 (s, 1 C), 48.50 (s, 1 C), 45.26 (s, 1 C), 45.26 (s, 1 C), 35.50 (s, 1 C).

1-(5-(2-chlorophenyl)-7,8-dimethoxy-3-(4-methoxyphenethyl)-3H-pyrazolo[3,4-c]isoquinolin-1-yl)-N,N-dimethylmethanamine (27)

To a solution of compound **12c** (40 mg, 0.01 mmol) in dried DMF in the presence of cesium carbonate (55 mg, 0.170 mmol) was added 4-(2-chloroethyl)anisole (14.5 mg, 0.170 mmol). After the mixture was stirred at room temperature for 1 h, the solvent was removed in vacuo. The residue was taken up in solution of saturated aqueous ammonium chloride and extracted with ethyl acetate twice. The combined extract was dried with anhydrous Na₂SO₄, filtered and evaporated. The residue was purified by silica gel column chromatography with MeOH:CHCl₃ (1%) to afford compound **27** as a transparent liquid. ¹H NMR (400 MHz, CDCl₃) δ 8.31 (s, 1 H), 7.60 - 7.55 (m, 1 H), 7.49 - 7.44 (m, 2 H), 7.43 - 7.40 (m, 1 H), 7.04 (m, J=8.70 Hz, 2 H), 6.91 (s, 1 H), 6.74 - 6.68 (m, 2 H), 4.77 (t, J=7.56 Hz, 2 H), 4.12 (s, 3 H), 3.95 (s, 2 H), 3.77 (s, 3 H), 3.73 (s, 3 H), 3.22 (t, J=7.33 Hz, 2 H), 2.39 (s, 6 H). ¹³C NMR (126 MHz, CDCl₃) δ ppm 158.05 (s, 1 C), 156.73 (s, 1 C), 153.29 (s, 1 C), 147.52 (s, 1 C), 138.85 (s, 1 C), 133.40 (s, 1 C), 131.42 (s, 1 C), 130.57 (s, 1 C), 129.88-129.86 (s, 5 C), 129.79 (s, 1 C), 129.78 (s, 1 C), 126.82 (s, 1 C), 118.86 (s, 1 C), 113.69 (s, 1 C), 113.69 (s, 1 C), 113.62 (s, 1 C), 108.03 (s, 1 C), 107.84 (s, 1 C), 56.05 (s, 1 C), 55.82 (s, 1 C), 55.17 (s, 1 C), 55.17 (s, 1 C), 48.51 (s, 1 C), 45.40 (s, 1 C), 45.25 (s, 1 C), 35.41 (s, 1 C).

3-(5-(3-chlorophenyl)-1-((dimethylamino)methyl)-7,8-dimethoxy-3H-pyrazolo[3,4-c]isoquinolin-3-yl)propanenitrile (29)

To a solution of compound **12a** (40 mg, 0.085 mmol) in dried DMF in the presence of cesium carbonate (55 mg, 0.170 mmol) was added 3-bromopropionitrile (23.2 mg, 0.170 mmol). After the mixture was stirred at room temperature for 1.5 h, the solvent was removed in vacuo. The residue was taken up in solution of saturated aqueous ammonium chloride and extracted with ethyl acetate twice. The combined extract was dried with anhydrous Na₂SO₄, filtered and evaporated. The residue was purified by silica gel column chromatography with MeOH:CHCl₃ (1%) to afford compound **29** as a white liquid (yield = 60%). ¹H NMR (400 MHz, CDCl₃) δ 8.35 (s, 1 H), 7.75 (dt, 1 H), 7.62 (ddd, 1 H), 7.55 - 7.50 (m, 2 H), 7.39 (s, 1H), 4.88 (t, 2 H), 4.14 (s, 3 H), 3.98 (s, 2 H), 3.87 (s, 3 H), 3.08 (t, 2 H), 2.43 (s, 6 H). ¹³C NMR (126 MHz, CDCl₃) δ ppm 157.30 (s, 1 C), 153.49 (s, 1 C), 147.80 (s, 1 C), 147.63 (s, 1 C), 141.63 (s, 1 C), 134.52 (s, 1 C), 129.94 (s, 1 C), 129.64 (s, 1 C), 128.98 (s, 1 C), 128.94 (s, 1 C), 128.94 (s, 1 C), 127.95 (s, 1 C), 118.60 (s, 1 C), 117.08 (s, 1 C), 108.27 (s, 1 C), 107.88 (s, 1 C), 105.51 (s, 1 C), 56.10 (s, 1 C), 55.89 (s, 1 C), 55.89 (s, 1 C), 45.31 (s, 1 C), 45.31 (s, 1 C), 42.37 (s, 1 C), 18.57 (s, 1 C).

1-(5-(3-chlorophenyl)-3-isobutyl-7,8-dimethoxy-3H-pyrazolo[3,4-c]isoquinolin-1-yl)-N,N-dimethylmethanamine (30)

To a solution of compound **12a** (40 mg, 0.1 mmol) in dried DMF in the presence of cesium carbonate (55 mg, 0.170 mmol) was added 1-bromo-2-methyl propane (23.2 mg, 0.170 mmol). After the mixture was stirred at room temperature for 1 h, the solvent was removed in vacuo. The residue was taken up in solution of saturated aqueous ammonium chloride and extracted with ethyl acetate twice. The combined extract was dried with anhydrous Na₂SO₄, filtered and evaporated. The residue was purified by silica gel column chromatography with MeOH:CHCl₃ (1%) to afford compound **30** as a yellow liquid. ¹H NMR (400 MHz, CDCl₃) δ 8.34 (s, 1 H), 7.73 (t, J=1.83 Hz, 1 H), 7.61 (m, 1 H), 7.53 - 7.48 (m, 2 H), 7.40 - 7.37 (m, 1 H), 4.41 - 4.36 (m, 2 H), 4.13 (s, 3 H), 3.95 (s, 2 H), 3.86 (s, 3 H), 2.39 (s, 7 H), 0.96 - 0.91 (m, 6 H). ¹³C NMR (126 MHz, CDCl₃) δ ppm 157.58 (s, 1 C), 153.54 (s, 1 C), 148.00 (s, 1 C), 147.70 (s, 1 C), 142.42 (s, 1 C), 141.85 (s, 1 C), 134.47 (s, 1 C), 130.01 (s, 1 C), 129.58 (s, 1 C), 128.87 (s, 1 C), 128.40 (s, 1 C), 128.03 (s, 1 C), 118.24 (s, 1 C), 108.15 (s, 1 C), 106.83 (s, 1 C), 103.99 (s, 1 C), 60.12 (s, 1 C), 56.21 (s, 1 C), 56.21 (s, 1 C), 55.90 (s, 1 C), 54.20 (s, 1 C), 54.20 (s, 1 C), 29.40 (s, 1 C), 20.08 (s, 1 C), 20.08 (s, 1 C).

1-(5-(3-chlorophenyl)-7,8-dimethoxy-3-(2-(1-methylpyrrolidin-2-yl)ethyl)-3H-pyrazolo[3,4-c]isoquinolin-1-yl)-N,N-dimethylmethanamine (31)

To a solution of compound **12a** (10 mg, 0.021 mmol) in dried DMF in the presence of cesium carbonate (14 mg, 0.045 mmol) was added 2-(2-bromoethyl)-1-methylpyrrolidine (5.8 mg, 0.043 mmol). After the mixture was stirred at room temperature for 1.5 h, the solvent was removed in vacuo. The residue was taken up in solution of saturated aqueous ammonium chloride and extracted with ethyl acetate twice. The combined extract was dried with anhydrous Na₂SO₄, filtered and

FULL PAPER

evaporated. The residue was purified by silica gel column chromatography with MeOH:CHCl₃ (1%) to afford compound **31** as a white liquid (yield = 62%) ¹H NMR (400 MHz, DMSO-d₆) δ 8.07 (s, 1 H), 7.76 (s, 1 H), 7.73 – 7.69 (m, 1 H), 7.65 – 7.60 (m, 2 H), 4.98 (t, 2 H), 4.01 (s, 3 H), 3.87 (s, 2 H), 3.75 (s, 3 H), 3.62 (s, 3 H), 3.15 (q, 2 H), 2.27 (s, 6 H), 2.18 – 1.63 (m, 6H).

1-(5-(4-chlorophenyl)-3-isobutyl-7,8-dimethoxy-3H-pyrazolo[3,4-c]isoquinolin-1-yl)-N,N-dimethylmethanamine (33)

To a solution of compound **12b** (40 mg, 0.1 mmol) in dried DMF in the presence of cesium carbonate (55 mg, 0.170 mmol) was added 1-bromo-2-methyl propane (23.2 mg, 0.170 mmol). After the mixture was stirred at room temperature for 1 h, the solvent was removed in vacuo. The residue was taken up in solution of saturated aqueous ammonium chloride and extracted with ethyl acetate twice. The combined extract was dried with anhydrous Na₂SO₄, filtered and evaporated. The residue was purified by silica gel column chromatography with MeOH:CHCl₃ (1%) to afford compound **33** as a pale-yellow liquid. ¹H NMR (400 MHz, CDCl₃) δ 8.34 (s, 1 H), 7.70 – 7.66 (m, 2 H), 7.57 – 7.52 (m, 2 H), 7.39 (s, 1 H), 4.37 (d, J=7.33 Hz, 2 H), 4.12 (s, 3 H), 3.95 (s, 2 H), 3.85 (s, 3 H), 2.53 – 2.33 (m, 7 H), 0.96 – 0.88 (m, 6 H). ¹³C NMR (126 MHz, CDCl₃) δ ppm 157.58 (s, 1 C), 153.54 (s, 1 C), 148.00 (s, 1 C), 147.70 (s, 1 C), 142.42 (s, 1 C), 141.85 (s, 1 C), 134.47 (s, 1 C), 130.01 (s, 1 C), 129.58 (s, 1 C), 128.87 (s, 1 C), 128.40 (s, 1 C), 128.03 (s, 1 C), 118.24 (s, 1 C), 108.15 (s, 1 C), 106.83 (s, 1 C), 103.99 (s, 1 C), 60.18 (s, 1 C), 56.21 (s, 1 C), 56.21 (s, 1 C), 55.91 (s, 1 C), 55.91 (s, 1 C), 54.20 (s, 1 C), 29.40 (s, 1 C), 20.05 (s, 1 C), 20.05 (s, 1 C).

Biological assay for opioid receptor agonism

The predicted compounds were tested for agonist activity using an intracellular calcium release assay. HEK/Ga15 stable cell line (Millipore) expressing Ga15 protein to measure intracellular Ca²⁺ ion release upon receptor activation was transfected with opioid receptor genes (μ-OR1 or κ-OR1). The compound solution was diluted with Ca²⁺ buffer solution to give 0.1% final concentration in cells. Positive controls such as DynorphinA for κ-OR agonist and DAMGO for μ-OR agonist were prepared same method of the compound. On the day before the assay, frozen cell was re-suspended in fresh media and seeded at 5*10⁴/well, 100mL/well in 96-well plate. Cells were cultured overnight at 37°C with 5% CO₂. The calcium dye was loaded into cells at 100 μL/well. The assay plates were incubated at 37°C for 2 h. Assay plates were then placed onto the FLIPR tetra fluorescence plate reader for treating 50 μL of the compounds solution and positive controls and measuring the changes of intracellular calcium efflux response to the opioid receptor activation. For each compound, concentration response profiles were established by measuring the fluorescence every second from ten seconds before treating compound for 60 seconds and determining the peak effect (maximum-minimum). A dose response curve was plotted with the change in Relative Fluorescence Units (ΔRFU) vs. concentration.

Biological assay for opioid receptor antagonism

The predicted compounds were tested for antagonist activity using an intracellular calcium release assay. HEK/Ga15 stable cell line (Millipore) expressing Ga15 protein to measure intracellular Ca²⁺ ion release upon receptor activation was transfected with opioid receptor genes (μ-OR1 or κ-OR1). The compound solution was diluted with Ca²⁺ buffer solution to give 0.1% final concentration in cells. For antagonist assay, on the day before the assay, frozen cell was re-suspended in fresh media and seeded at 5*10⁴/well, 100 μL/well in 96-well plate. Cells were cultured overnight at 37°C with 5% CO₂. After 1 h the calcium dye loaded into the wells, each compound was treated for 10 μM of working concentration. The assay plates were incubated at 37°C for additional 1 h. Assay plates were then placed onto the FLIPR tetra fluorescence plate reader for treating 50 μL of the 0.08 mg/mL dynorphin solution for κ-OR 1 (or 0.2 mg/mL DAMGO for intracellular Ca²⁺ ion release upon receptor activation was transfected with opioid receptor genes (μ-OR 1) and measuring the changes of intracellular calcium efflux response to the opioid receptor activation. For each compound, relative fluorescence units (RFU) were established by measuring the fluorescence every second from ten seconds before treating agonist for 60 seconds and determining the peak effect (maximum-minimum). %inhibition was calculated with mean value of background treated (100%) and agonist only treated (0%).

β-arrestin recruitment assay

PathHunter GPCR β-arrestin recruitment assays are whole-cell functional assays that directly measure GPCR activity by detecting the interaction of β-arrestin with activated GPCR using β-galactosidase (β-gal) enzyme fragment complementation. Assays are proceeded using the PathHunter β-Arrestin GPCR Cell Lines and specific PathHunter Detection, Cell Plating (CP) reagents. Cells are harvested using selective cell detachment reagent and added CP reagent. Cell suspension were centrifuged for 3 minutes at 1500 RPM at room temperature and supernatant were removed. (Resuspend cells of CP reagent at a concentration of 2.5x [10] ⁵ cells / mL). Transfer 20 μL of the cell suspension to each well of micro plate and incubate for overnight at 37°C, 5% CO₂. Dissolve each agonist compound dissolved in DMSO to the desired concentration, add 5 μl to each well, and incubate at 37°C for 90 minutes. Prepare the PathHunter detection reagent, add 12 μL to the each well, and incubate at room temperature for 60 mins. Assays plates were placed on to the luminescence plate reader and read chemiluminescent signal.

Animal preparation for Formalin test

All experimental protocols were reviewed and approved by the Institutional Animal Care and Use Committee of Chonnam National University. Adult male Sprague-Dawley rats (250 - 300 g) were used in the present study. Animals were housed four to a cage and kept in a vivarium maintained at 22°C with a 12 h: 12 h alternating light/dark cycle. All rats received food and water ad libitum. All test drugs were intrathecally administered. Thus, rats were implanted with intrathecal catheters under sevoflurane anesthesia. An 8.5-cm-long polyethylene-10catheter was advanced caudally, through an incision in the cisternal membrane, to the thoracolumbar level of the spinal cord. The exterior portion of the catheter was secured at the skull via subcutaneous tunnelling, and was closed with a 30-gauge wire. The skin was sutured

FULL PAPER

with 3-0 silk. After catheter implantation, rats were housed in individual cages. Only animals with no evidence of neurological deficits developing after catheter implantation were included in the present study; such rats were housed individually. The behavioral study was performed 5 days after intrathecal catheterization.

Formalin test

The formalin test was carried out as a nociceptive behavioral test. Subcutaneous injection of 50 μ L of 5% formalin solution was performed into the plantar surface of the hind paw using a 30-gauge needle. The rat displayed inherent abnormal behavior following formalin injection as follows a rapid and brief withdrawal or flexion of the injected paw. This peculiar behavior was called as flinching response and regarded as a painful response. Such pain behavior was therefore quantified by periodically counting the number of flinching of the injected paw. The number of flinches was counted for 1 min periods from 1 to 2 min, 5 to 6 min and every 5 min from 10 to 60 min. Because of the biphasical pattern of the flinching response after formalin injection, the interval from 0-9 min and the interval from 10-60 min were divided into phase 1 and phase 2 of the formalin test, respectively. Upon completion the test, the rats were euthanized with volatile anesthetics.

Scream

SCREAM^[23] was developed to find the optimum side-chain conformations of residues to avoid bad conflicts for residues on different backbones while optimizing favourable HB and SB interactions.

Acknowledgements

This work was supported by the GIST-Caltech Research Collaboration Project through a grant provided by GIST for 2016-2019. It was also funded by grants from the China Scholarship Council and by gifts to the Materials and Process Simulation Centre. The computational resources were provided a DURIP-ONR grant to Goddard.

Keywords: opioid • G_i-biased agonist • virtual screening • protein construction • R-group screening

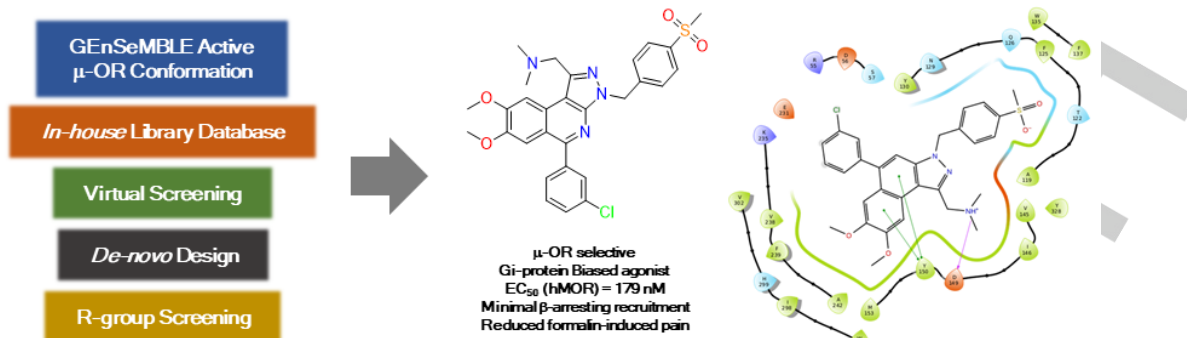
References:

- [1] K. M. Raehal, C. L. Schmid, C. E. Groer, L. M. Bohn, *Pharmacological reviews* **2011**, *63*(4), 1001-1019.
- [2] R. P. Mattick, C. Breen, J. Kimber, M. Davoli, *Cochrane database of systematic reviews* **2014**(2).
- [3] R. Payne, S. D. Mathias, D. J. Pasta, L. A. Wanke, R. Williams, R. Mahmoud, *Journal of clinical oncology* **1998**, *16*(4), 1588-1593.
- [4] C. f. S. A. Treatment, **2005**.
- [5] M. Camilleri, *The American journal of gastroenterology* **2011**, *106*(5), 835.
- [6] aD. G. Soergel, R. A. Subach, N. Burnham, M. W. Lark, I. E. James, B. M. Sadler, F. Skobieranda, J. D. Violin, L. R. Webster, *PAIN@* **2014**, *155*(9), 1829-1835; bE. J. Whalen, S. Rajagopal, R. J. Lefkowitz, *Trends in molecular medicine* **2011**, *17*(3), 126-139.
- [7] N. K. Singla, A. Senagore, E. R. Viscusi, D. A. Burt, D. Soergel, *The Spine Journal* **2017**, *17*(10), S207.

- [8] aE. R. Viscusi, L. Webster, M. Kuss, S. Daniels, J. A. Bolognese, S. Zuckerman, D. G. Soergel, R. A. Subach, E. Cook, F. Skobieranda, *Pain* **2016**, *157*(1), 264-272; bF. Skobieranda, N. Singla, D. Burt, D. Soergel, *The Journal of Pain* **2017**, *18*(4), S31-S32.
- [9] A. Manglik, H. Lin, D. K. Aryal, J. D. McCorvy, D. Dengler, G. Corder, A. Levit, R. C. Kling, V. Bernat, H. Hübner, *Nature* **2016**, *537*(7619), 185.
- [10] G. L. Thompson, J. R. Lane, T. Coudrat, P. M. Sexton, A. Christopoulos, M. Canals, *Biochemical pharmacology* **2016**, *113*, 70-87.
- [11] S. M. DeWire, D. S. Yamashita, D. H. Rominger, G. Liu, C. L. Cowan, T. M. Graczyk, X.-T. Chen, P. M. Pitis, D. Gotchev, C. Yuan, *Journal of Pharmacology and Experimental Therapeutics* **2013**, *344*(3), 708-717.
- [12] aL. M. Bohn, R. R. Gainetdinov, T. D. Sotnikova, I. O. Medvedev, R. J. Lefkowitz, L. A. Dykstra, M. G. Caron, *Journal of Neuroscience* **2003**, *23*(32), 10265-10273; bA. Kliewer, F. Schmiedel, S. Sianati, A. Bailey, J. Bateman, E. Levitt, J. Williams, M. Christie, S. Schulz, *Nature communications* **2019**, *10*(1), 367.
- [13] aR. Abrol, A. R. Griffith, J. K. Bray, W. A. Goddard, 3rd, *Methods in molecular biology* **2012**, *914*, 237-254; bR. Abrol, S. K. Kim, J. K. Bray, B. Trzaskowski, W. A. Goddard, 3rd, *Methods in enzymology* **2013**, *520*, 31-48; cR. Abrol, J. K. Bray, W. A. Goddard, 3rd, *Proteins* **2011**; dJ. K. Bray, R. Abrol, W. A. Goddard, 3rd, B. Trzaskowski, C. E. Scott, *Proceedings of the National Academy of Sciences of the United States of America* **2014**, *111*(1), E72-78.
- [14] aS. K. Kim, L. Riley, R. Abrol, K. A. Jacobson, W. A. Goddard III, *Proteins: Structure, Function, and Bioinformatics* **2011**, *79*(6), 1878-1897; bL. Charlier, J. Topin, C. Ronin, S.-K. Kim, W. A. Goddard, R. Efremov, J. Golebiowski, *Cellular and molecular life sciences* **2012**, *69*(24), 4205-4213; cA. Kirkpatrick, J. Heo, R. Abrol, W. A. Goddard, *Proceedings of the National Academy of Sciences* **2012**, *109*(49), 19988-19993; dJ. Tan, R. Abrol, B. Trzaskowski, W. A. Goddard III, *Journal of chemical information and modeling* **2012**, *52*(7), 1875-1885; eR. Berro, A. Yasmeen, R. Abrol, B. Trzaskowski, S. Abi-Habib, A. Grunbeck, D. Lascano, W. A. Goddard, 3rd, P. J. Klasse, T. P. Sakmar, J. P. Moore, *Journal of virology* **2013**, *87*(12), 6569-6581; fC. E. Scott, R. Abrol, K. H. Ahn, D. A. Kendall, W. A. Goddard III, *Protein Science* **2013**, *22*(1), 101-113.
- [15] W. M. Huang, A.; Venkatakrishnan, A.J.; Laeremans, T.; Feinberg, E.N.; Sanborn, A.L.; Kato, H.E.; Livingston, K.E.; Thorsen, T.S.; Kling, R.C.; Granier, S.; Gmeiner, P.; Husbands, S.M.; Traynor, J.R.; Weis, W.I.; Steyaert, J.; Dror, R.O.; Kobilka, B.K., *Nature* **2015**, *524*, 315-321.
- [16] H. Wu, D. Wacker, M. Mileni, V. Katritch, G. W. Han, E. Vardy, W. Liu, A. A. Thompson, X.-P. Huang, F. I. Carroll, *Nature* **2012**, *485*(7398), 327.
- [17] A. Manglik, Kruse, A.C., Kobilka, T.S., Thian, F.S., Mathiesen, J.M., Sunahara, R.K., Pardo, L., Weis, W.I., Kobilka, B.K., Granier, S., *Nature* **2012**, *485*, 321-323.
- [18] G. F. Fenalti, P.M.; Katritch, V.; Huang, X.P.; Thompson, A.A.; Cherezov, V.; Roth, B.L.; Stevens, R.C., *Nature* **2014**, *506*, 191-196.
- [19] A. A. L. Thompson, W.; Chun, E.; Katritch, V.; Wu, H.; Vardy, E.; Huang, X.P.; Trapella, C.; Guerrini, R.; Calo, G.; Roth, B.L.; Cherezov, V.; Stevens, R.C., *Nature* **2012**, *485*, 395-399.
- [20] Q. Li, S.-K. Kim, W. A. Goddard III, G. Chen, H. Tan, *J. Chem. Inf. Model.* **2015**, *55*(3), 614-627.
- [21] V. Cvicsek, W. A. Goddard III, R. Abrol, *PLoS computational biology* **2016**, *12*(3), e1004805.
- [22] A. Venkatakrishnan, X. Deupi, G. Lebon, C. G. Tate, G. F. Schertler, M. M. Babu, *Nature* **2013**, *494*(7436), 185.
- [23] V. W. T. Kam, W. A. William A. Goddard III, *J. Chem Theory Comput.* **2008**, *4*(12), 2160-2169.
- [24] S. L. Mayo, B. D. Olafson, W. A. Goddard III, *J Phys Chem.* **1990**, *94*(26), 8897-8909.

FULL PAPER

Entry for the Table of Contents



To discovery of G_i-protein biased opioid receptor agonist, we build active homology models from a vast number of potential packings (10 trillion) of opioid receptors and processed structure-based drug design. Novel pyrazolo[3,4-c]isoquinoline derivatives were synthesized through the step-by-step computational optimization and the compound 19 displayed a selective activation of human mu opioid receptor with minimal β-arrestin recruitment.